

Nathan, Horvitz, He, Kuparinen, Schurr and Katul

Spread of North American wind-dispersed trees in future environments

Supplementary Material

Appendix 1. Modeling the spread rate of wind-dispersed plants.

(Table S1, Figures S1, S2, S3, S4 and S5).

Appendix 2. Determinants of spread rate in North American wind-dispersed tree species.

(Tables S2, S3 and S4, Figures S6 and S7).

Appendix 3. Complementary analyses of current vs. future spread of North American wind-dispersed tree species.

(Tables S5 and S6, Figure S8).

Appendix 1. Modeling the spread rate of wind-dispersed plants

I. Basic spread rate calculations

The scale (μ) and shape (γ) parameters of the WALD dispersal kernel (Katul *et al.* 2005) are calculated as

$$\mu = \frac{p_r h_t \bar{u}}{v_t}$$
$$\gamma = \frac{\bar{u} (p_r h_t)^2}{2 \kappa h_t \sigma_w},$$

where \bar{u} is the mean windspeed (obtained by averaging over all turbulent time scales - and this averaging is usually on the order of 0.5 to 1 hour); σ_w is the standard deviation of the vertical velocity of the air; p_r is the proportional height of seed release from h_t , the average tree height; v_t is seed terminal falling velocity and κ is a turbulence coefficient assumed here to be equal to 0.4 (Katul *et al.* 2005). The parameters \bar{u} and σ_w are computed from an analytical model described in Massman & Weil (1999). This model is a second-order moment-closure scheme that computes the dimensionless velocity statistics inside the canopy from leaf area density and foliage drag coefficient (Massman & Weil 1999; Katul *et al.* 2005). The canonical form of the one-dimensional WALD dispersal distance kernel is given by

$$f_{wald}(\rho) = \sqrt{\frac{\gamma}{2\pi\rho^3}} \exp\left[-\frac{\gamma(\rho - \mu)^2}{2\mu^2\rho}\right],$$

where $f_{wald}(\rho)$ is the probability density of a seed to arrive at a distance ρ from the source (the mother plant).

The marginal effective dispersal distance probability density function $f_{effective}(x)$ calculates the probability density of a seed to arrive to a point (x, y) and survive to maturity. To account for two-dimensional effects of seed deposition at the ground, we align x along the mean wind (or longitudinal) direction and y (or lateral) orthogonal to this direction at the ground. In this

coordinate system, the seed source is situated at $(0,0)$, where $(x, y) \in \mathbb{R}^2$. Hence, to calculate $f_{effective}(x)$ it becomes necessary to integrate the WALD dispersal distance kernel that a seed arrives to distance $\sqrt{x^2 + y^2}$, divided by the perimeter of a circle with radius $\sqrt{x^2 + y^2}$ and multiplied by the survival ($\varphi(\rho)$, section IV below) at distance $\rho = \sqrt{x^2 + y^2}$, over all points in the form (x, y) (where integration variable y goes from $-\infty$ to ∞), that is

$$f_{effective}(x) = \int_{-\infty}^{\infty} \left(\frac{f_{wald}(\sqrt{x^2 + y^2})}{2\pi\sqrt{x^2 + y^2}} \varphi(\sqrt{x^2 + y^2}) \right) dy.$$

Note that the above formulation assumes isotropic dispersal from a single tree (the farthest, see below); that is, seeds are dispersed (and the population spreads) to all directions with no particular bias. In cases of non-uniform distribution of the mean wind direction leading to anisotropic dispersal, spread rate in certain direction(s) will be faster than under the isotropic assumption, but in other directions it will be slower. Therefore, assessing spread rate under anisotropic dispersal requires information on the distribution of wind direction (and speed) in relation to the direction of the environmental change (e.g., poleward during global warming or large-scale glacial retreat). This complexity is yet to be investigated in future studies.

The marginal effective dispersal distance probability density function $f_{effective}$ is now used to predict population spread with a model similar to the invasion by extremes model of Clark *et al.* (2001). Yet, in contrast to this model, our spread model does not assume that all seeds are dispersed at the same mother plant age (the generation time). Instead, it describes variability in the mother plant age at seed dispersal, t . Hence, the state variable of our spread model is not the mother-to-offspring dispersal distance x (as in Clark *et al.* 2001), but the mother-to-offspring spread rate $c = x/t$. Under the simplifying assumption that t is uniformly distributed between t_M and t_L , the ages of first (“maturation”) and last (“longevity”)

reproduction, we obtain the unnormalized kernel of mother-to-offspring spread rate by integrating $f_{effective}$ over the reproductive lifespan of the species

$$f_{reprolife}(c) = \int_{t_M}^{t_L} f_{effective}(tc) dt .$$

To obtain a normalized probability density function of mother-to-offspring spread rate f_{speed} , we normalize with the probability of a dispersed seed to survive to maturity (r),

$$f_{speed}(c) = \frac{f_{reprolife}(c)}{r} ,$$

where r is calculated by integrating the unnormalized spread kernel over all possible speeds

$$r = \int_{-\infty}^{\infty} f_{reprolife}(c) dc .$$

The fact that speed spans both negative and positive values can be attributed to fluctuations in mean wind direction occurring every 0.5 hours.

The net reproductive rate (R_0), the total number of seeds that dispersed and survived to maturity during the reproductive lifespan of a tree, equals the annual fecundity in years of high seed crop (β) times the probability of a single seed to survive (r) times the reproductive lifespan divided by mean interval between high seed crop years (t_{IC}), assuming seed rain in low seed crop years is negligible. We thus have

$$R_0 = \frac{\beta r (t_L - t_M)}{t_{IC}} .$$

The population-level spread rate in a single generation C is a random variable denoting the maximum of the R_0 mother-to-offspring spread rates for the offspring produced by the farthest forward tree in the population. In analogy to Clark *et al.* (2001, equation 1), the probability density of this extreme spread rate C can be calculated using order statistics

$$f_{spread}(c) = R_0 f_{speed}(c) \left[\int_{-\infty}^c f(y) dy \right]^{R_0 - 1} .$$

Thus, the asymptotic spread rate of the population (c^*) is the expectation of C :

$$c^* = E[C] = \int_{-\infty}^{\infty} c f_{spread}(c) dc .$$

Note that in the special case of all seeds being produced at average generation time $T = t_M = t_L$, our spread model simplifies to the model of Clark *et al.* (2001).

II. A Weibull-based mixture of WALD kernels

The two-parameter Weibull distribution, the most widely used for the \bar{u} probability distribution (Burton et al. 2001), has the form of

$$f_{weibull}(\bar{u}) = \frac{w_\beta}{w_\alpha} \left(\frac{\bar{u}}{w_\alpha} \right)^{w_\beta - 1} \mathbf{exp} \left[- \left(\frac{\bar{u}}{w_\alpha} \right)^{w_\beta} \right],$$

where w_α and w_β are scale and shape parameters, respectively. To describe the process of seed dispersal by winds with Weibull-distributed speeds, we implement the Thompson & Katul's (2008) approach. The Weibull distribution was divided into $N = 20$ equal-probability bins (see Figure S1), and run the spread rate calculations as described in section I with the midpoint value (of the probability, not the range) of each bin (\bar{u}_i) as the characteristic windspeed (Figure S1). Thus, the overall spread rate is the average of all bins

$$c^* = \frac{\sum_{i=1}^N c_{\bar{u}_i}}{N} .$$

For calculations with a seed abscission threshold windspeed, the same method was implemented, but the bins were modified to correspond to a thresholded windspeed.

III. Future windspeed scenarios

To assess the current windspeed distribution over North America, we analyzed 21-year (1979-1999) 3-hourly surface wind records from 776 weather stations (Figure S2; see He *et al.* 2010 for details). We fitted the surface windspeed data to a Weibull distribution following the

common practice in this field (Burton *et al.* 2001, He *et al.* 2010) and previous wind dispersal studies (Nathan & Katul 2005, Thompson & Katul 2008).

To assess the windspeed distribution expected for the middle of the current century (the future timeframe in our study), we combined two complementary methods – analysis of recent trends and forecasting by regional climate models.

First, measurements of 10-m surface windspeed show a negative linear trend of $[-0.00714, -0.00261]$ $\text{m s}^{-1} \text{ yr}^{-1}$ over most of Canada during the last five decades (1953-2006), with a small positive trend of $0.00316 \text{ m s}^{-1} \text{ yr}^{-1}$ in the Arctic (Wan *et al.* 2010); linear extrapolation to the middle of the current century yields changes of -7% to 3% in windspeed over Canada. A comprehensive analysis of eight datasets including observations, reanalysis, and regional climate model wind products revealed a declining mean surface windspeed of similar magnitude over most regions of US (Pryor *et al.* 2009).

Second, we run the Canadian Regional Climate Model (CRCM) version 4 (CRCM4), driven by the third generation Canadian Global Circulation Model (CGCM3) under the A2 emissions scenario, to predict lower and upper bounds for the future timeframe (2049-2069) over the relevant parts of North America, excluding Arctic zones well beyond the current tree line. Altogether, the simulations predict both negative and positive changes in surface windspeed (Figure S2). Overall, mean surface windspeed over the entire North America is predicted to change only slightly (overall mean 1%), with slightly declining windspeeds over most of the area including the western part of US and Canada and forest-dominated southwest of US. This spatial pattern is consistent with historical trend of surface windspeed in the past several decades over Canada (Wan *et al.* 2010) and US (Pryor *et al.* 2009). Increases in windspeed are predicted in central US and at high latitude regions, consistent with observed trend (Wan *et al.* 2010). For the future timeframe of our study, the Weibull scale parameter is

within [-4%, +6%] with an overall mean change 1%, and the shape parameter is within [-6%, +6%] with an overall mean change 0.7% (Figure S3).

In summary, combining the two methods yielded a lower -7% bound and an upper +6% bound for the proportional present-to-future change in mean surface windspeed.

It is important to stress that our future timeframe (2049-2069) for windspeed predictions is consistent with the predicted timeframe of the elevated CO₂ concentrations applied in the FACE experiments (~550 ppm) under IPCC SRES A2 emissions scenario (Nakišenoviš *et al.* 2000). Note that our CRCM4-CGCM3 simulations are also under the A2 scenario. A2 is one of the most “pessimistic” scenarios, assuming lack of integration among countries, continuously increasing human population at relatively high rate in a less ecologically-friendly world, compared to other major scenarios (Nakišenoviš *et al.* 2000). Thus, the selection of A2 scenario matches our goal of assessing the upper bound of tree spread in considerably altered environments in the future. How sensitive are our estimates to different emission scenarios is open for future studies.

Because the Weibull probability distribution is fitted to data from meteorological stations at 10 m height usually at open grasslands, we need to convert it to wind distributions above a forested landscape. This conversion is required given the logarithmic dependence of mean wind on height well above the canopy for near-neutral atmospheric conditions. For a given mean windspeed in grassland \bar{u}_{grass} sampled at $z = 10$ m height, the friction velocity (a measure of the ground shear stress) can be estimated from the log-law as

$$\bar{u}_{grass} = \frac{u_{*grass}}{K} \ln\left(\frac{z}{z_0}\right)$$

where u_* is the friction velocity, and K is the Von Karman constant (0.4). Assuming the canopy grass height $h_c = 1$ m and the momentum roughness length $z_0 \approx 0.1h_c$, then at $z = 10$ m

$$u_{*grass} = \frac{K\bar{u}_{grass}}{\ln\left(\frac{10}{0.1}\right)}.$$

From sonic anemometry data reported in Stoy *et al.* (2006), the expected enhancement in u_* above the forest when compared to the grassland due to its rougher z_o is

$$\frac{u_{*forest}}{u_{*grass}} = \frac{0.38}{0.17}$$

resulting in

$$\bar{u}_{forest} = u_{*forest} \bar{u}_{MW},$$

where \bar{u}_{MW} is the normalized \bar{u} derived from the Massman-Weil model (Massman & Weil, 1999).

IV. Survival data and survival function

The term “survival”, as used here and in the main text, refers to the probability of a dispersed seed to survive as a seed, germinate, survive and develop through subsequent stages (e.g., seedling, sapling) until it becomes a reproductive tree. Seed-to-adult survival probabilities have been rarely quantified for trees in natural conditions, and most of these few estimates are based on relatively short-term estimates. In one of the most comprehensive studies of seed and seedling survival of temperate trees, De Steven (1991a,b) examined seedling emergence and 3-yr seedling survival of six North American wind-dispersed tree species (all but one are included our selected 12 species) in field conditions, revealing average survival probability of 0.018 (range 0.000-0.061). The fraction of seedling emerged, however, was reported as total results of a 2x2 experimental design manipulating seed predators and competitors. Therefore, only one of the four treatment combinations (both natural predators and competitors not excluded) is relevant to assess seed survival in natural settings. Seedling emergence was significantly lower in this treatment combination compared to other combinations. Survival

probabilities estimates based on this treatment alone (values extracted visually from Figures 2 and 3 in De Steven 1991a) are roughly one order of magnitude lower, with mean and range of approximately ~0.002 (0.000-0.020). Accounting for mortality after 3 years and until maturation (5-50 years, Table 1 and Table S2 in Appendix 2), would further lower this survival estimate. Seed-to-adult survival under natural conditions is therefore very low in trees in general (Nathan *et al.* 2000, Terborgh *et al.* 2002; see next paragraph), and in North American wind-dispersed species in particular.

Survival is assumed to increase with distance from the mother plant since pathogens, seed predators and/or seedling herbivores are attracted to the seed source (Janzen 1970). Drastic increase in survival, extending 3-5 orders of magnitude over a few tens of meters, were found for trees in a tropical forest in Peru (Terborgh *et al.* 2002) and a Mediterranean forest in Israel (Nathan *et al.* 2000). However, beyond a certain distance, spatial autocorrelation effects of abiotic are expected to generate an opposing pattern, since more distant habitats are less similar and hence less suitable than nearby habitats (Nathan 2006; see main text for more details). A logical portray of spatially variable survival is thus an asymmetric hump-shaped function. We selected the log-logistic function

$$\varphi(\rho) = \lambda \frac{\left(\frac{\rho}{\varphi_\alpha} \right)^{\varphi_\beta - 1}}{\left[1 + \left(\frac{\rho}{\varphi_\alpha} \right)^{\varphi_\beta} \right]^2},$$

where φ_α and φ_β are the scale and shape parameters, respectively, and different mean survival values are achieved by changing the value of the dummy multiplier λ . For a given φ_β and a required mode (m), the survival scale parameter is

$$\varphi_\alpha = \frac{m}{\left(\frac{\varphi_\beta - 1}{\varphi_\beta + 1}\right) \frac{1}{\varphi_\beta}}$$

For $0 < \varphi_\beta < 1$, $m = 0$ and the function monotonically declines; for $\varphi_\beta > 1$, the function is hump-shaped. We used $\varphi_\beta = 1.5$ and $m = 100$ m for all calculations in this study (Figure S4). To ensure the same overall mean survival (Φ) for both spatially variable and uniform survival functions, we a-priori limited our spatial domain to 10 km, the lowest limit in the form of 10^n (where $n \in \mathbb{N}$) to yield deviations smaller than 1% in spread rate compared to calculation of no limited spatial domain (i.e., between 0 and infinity). We used six different values for Φ , decreasing in six orders of magnitude from 0.024 to 0.00000024, calculated as

$$\Phi = E[\varphi(\rho)] = E \left[\lambda \frac{\frac{\varphi_\beta \left(\frac{\rho}{\varphi_\alpha}\right)^{\varphi_\beta - 1}}{\varphi_\alpha \left(\frac{\rho}{\varphi_\alpha}\right)}}{\left[1 + \left(\frac{\rho}{\varphi_\alpha}\right)^{\varphi_\beta}\right]^2} \right] = E \lambda \frac{\frac{\varphi_\beta \left(\frac{\rho}{\varphi_\alpha}\right)^{\varphi_\beta - 1}}{\varphi_\alpha \left(\frac{\rho}{\varphi_\alpha}\right)}}{\left[1 + \left(\frac{\rho}{\varphi_\alpha}\right)^{\varphi_\beta}\right]^2}$$

To adjust the function for a desired overall mean survival Φ , one should assign λ as

$$\lambda = \frac{\Phi \left[1 + \left(\frac{\rho}{\varphi_\alpha}\right)^{\varphi_\beta}\right]^2}{\frac{\varphi_\beta \left(\frac{\rho}{\varphi_\alpha}\right)^{\varphi_\beta - 1}}{\varphi_\alpha \left(\frac{\rho}{\varphi_\alpha}\right)}}$$

V. Stochastic survival and the synchronization assumption

To examine the effects of stochastic spatiotemporal variation in post-dispersal mortality factors and establishment conditions, we randomly varied survival probability with distance from the source tree. Preserving the important advantage of the IBE model of much faster

computation compared to simulation models requires the use of a single survival function. Therefore, once a stochastic (or hump-shaped) survival function is randomly selected, its structure is maintained across generations. Yet, this practice necessitates that survival probability in a particular location is synchronized according to the distance from the current farthest individual. Thus, a site located, say, 5 km from the farthest individual in generation i will have a different survival probability in generation $i+1$, because the farthest individual is now, say, only 1 km from this site. The unrealistic synchronization assumption holds for both the hump-shaped and the stochastic survival functions and is obviously irrelevant for uniform survival; yet, the assumption of uniform survival itself is highly unrealistic.

To examine how biased is the predicted spread-rate due to the synchronization assumption, we calculated spread rate for a large number of different realizations of the stochastic survival function, compared to the one predicted for (a) spatially uniform and (b) hump-shaped survival, of the same mean. This practice adds a stochastic temporal (inter-generational) component to the spatial variation depicted by this stochastic survival function.

We found that the 95% confidence intervals around the corresponding (with the same mean) case of invariant survival are rather narrow, in the order of $\pm 10 \text{ m yr}^{-1}$ at the most (Figure S5). For the relatively fast spread rates predicted if dispersal occurs only in strong winds, the lower 95% confidence intervals are still much faster than the corresponding case of hump-shaped survival (Figure S5). Given the critical importance of survival in determining spread rate (see main text), a model implementing stochasticity in survival in space and time could have predicted a very different spread rate for a specific case (species and environment) than the same model assuming invariant survival or a fixed spatial structure. Yet, the lower and upper bounds of the mean spread rate of a typical North American of wind-dispersed tree species, and the much slower spread under hump-shaped compared to uniform survival, appear rather robust to the inclusion or exclusion of spatial stochasticity in survival.

Table S1. Summary of symbols

Symbol	Parameter	Type/Units
c	Spread rate	m yr^{-1}
C	Farthest forward spread rate	m yr^{-1}
c^*	Asymptotic spread rate	m yr^{-1}
$f_{\text{effective}}(x)$	Marginal effective dispersal distance function	
$f_{\text{speed}}(c)$	Marginal effective dispersal speed kernel	pdf
$f_{\text{spread}}(c)$	Spread rate kernel	pdf
$f_{\text{reprolife}}(c)$	Marginal effective dispersal speed function during the reproductive lifespan	
$f_{\text{wald}}(\rho)$	One-dimensional WALD dispersal distance kernel	pdf
$f_{\text{weibull}}(\bar{u})$	Two-parameter Weibull distribution	pdf
h_c	Mean forest canopy height	m
h_t	Mean tree height	m
K	Von-Karman constant	
p_r	Proportional height of seed release	%
r	The probability of a dispersed seed to survive to maturity	%
R_0	Net reproductive rate	# individuals
t_{IC}	Mean interval between good seed crop years	yr
t_L	Mean age at last reproduction (“maturity”)	yr
t_M	Mean age at first reproduction (“longevity”)	yr
\bar{u}	Mean horizontal windspeed	m s^{-1}
u_*	Friction velocity	m s^{-1}
U_r	Seed abscission minimum threshold windspeed	m s^{-1}
v_t	Mean seed terminal falling velocity	m s^{-1}
w_α	Weibull scale parameter	m s^{-1}
w_β	Weibull shape parameter	
(x, y)	Cartesian coordinates with seed source at (0,0)	m
β	Annual fecundity (seeds released in a good seed crop year)	# seeds
γ	WALD shape parameter	
κ	Turbulence coefficient	
μ	WALD scale parameter	
ρ	Euclidean distance from the seed source	m
σ_w	Standard deviation of vertical wind velocity	m s^{-1}
$\varphi(\rho)$	Survival function	
φ_α	Survival scale parameter	
φ_β	Survival shape parameter	
Φ	Mean survival over all space	%

Figure S1. Dividing a windspeed Weibull probability density to 20 equal-probability bins.

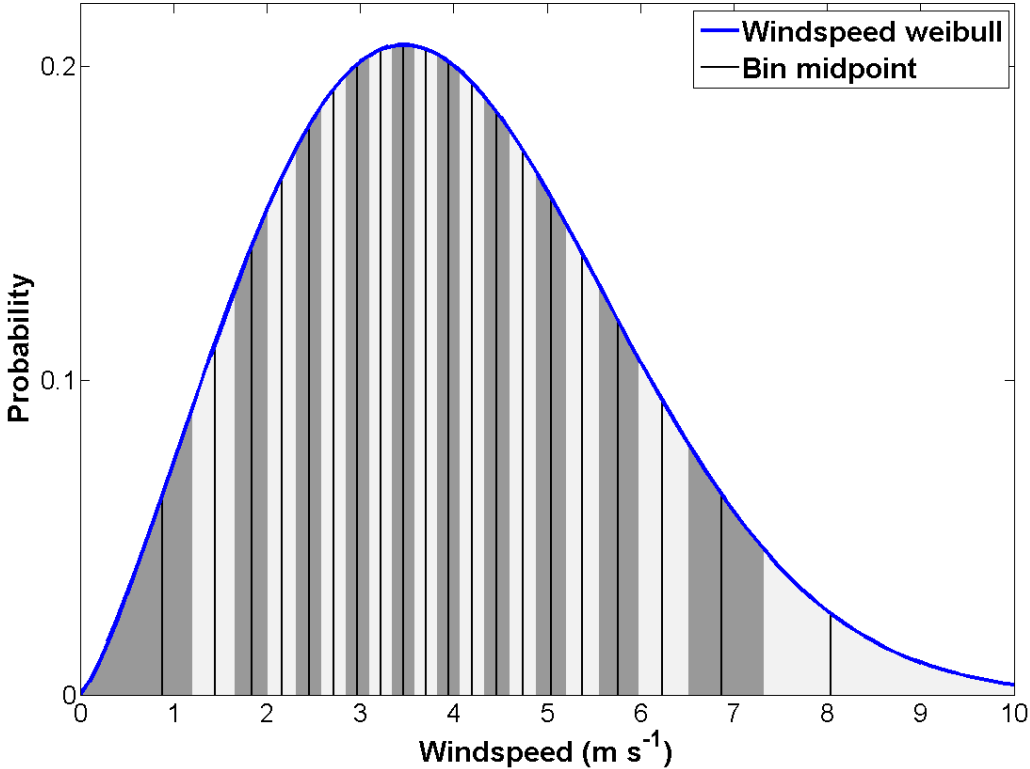


Figure S2. Current and predicted future surface windspeed over North America. The mean (left column) and standard deviation (right column) surface windspeed (m s^{-1}), based on data from weather station records (upper row) and from results of CRCM4 simulations for the present (middle row) and the middle (2049-2069) of the current century (lower row).

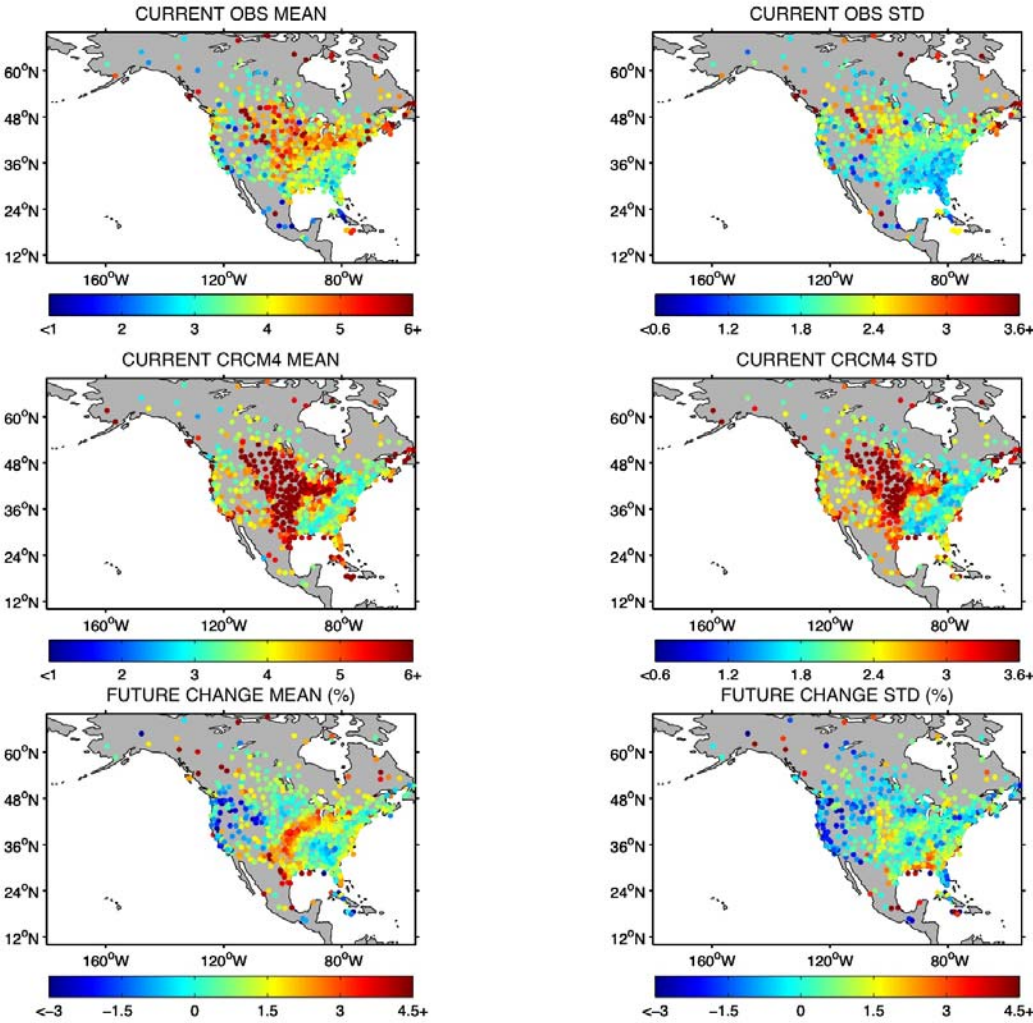


Figure S3. Current and predicted future surface wind statistics over North America. The scale (left column) and shape (right column) parameters of a Weibull distribution fitted to surface windspeed (m s^{-1}), based on data from weather station records (upper row) and from results of CRCM4 simulations for the present (middle row) and the middle (2049-2069) of the current century (lower row).

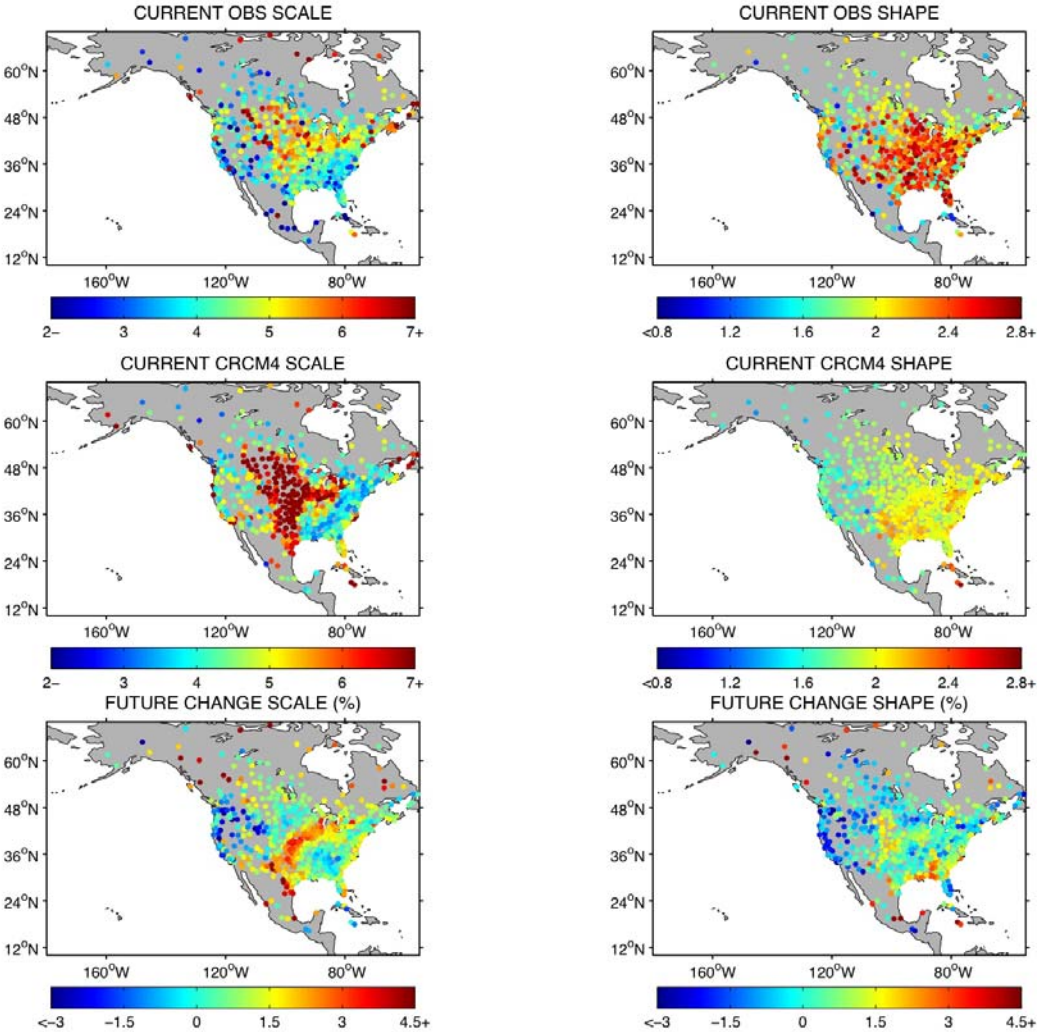


Figure S4. An illustrative log-logistic function (blue) used to describe spatially variable (hump-shaped) survival. The uniform survival function (red) has the same overall mean ($\Phi = 0.0024$) of the spatially variable one. Shape and scale parameters are 1.5 and 292.4, respectively, survival mode is 100 m and maximum survival is 0.05.

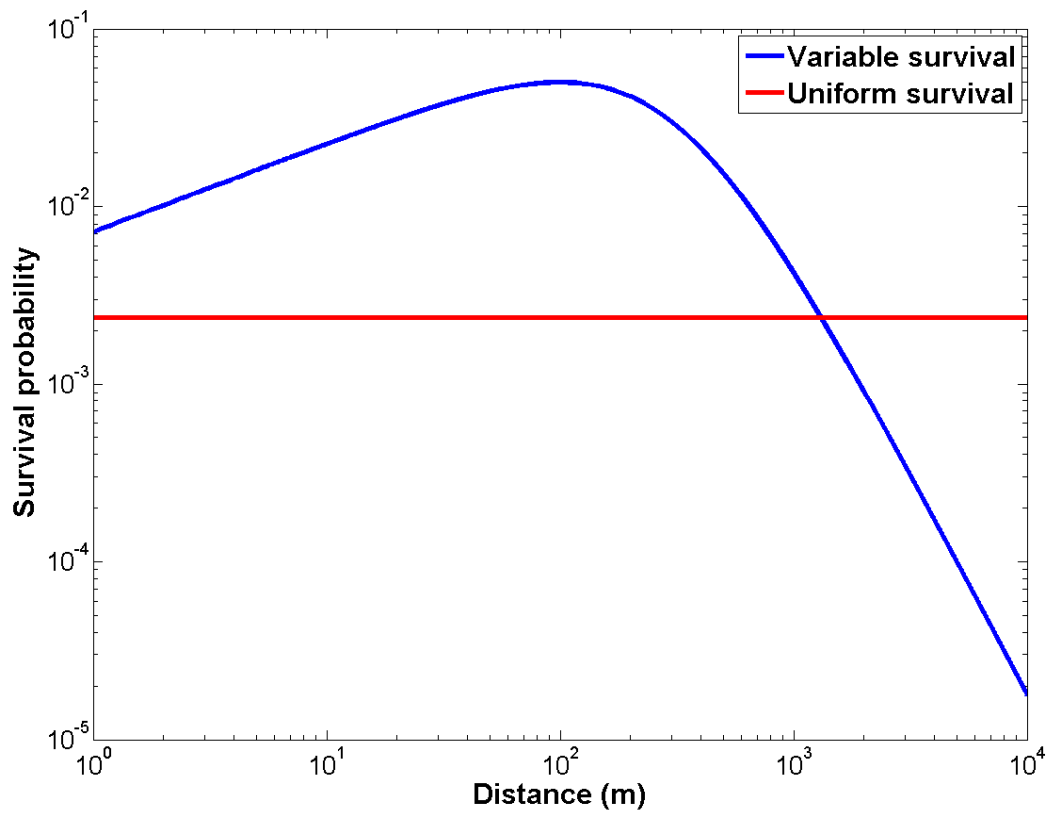
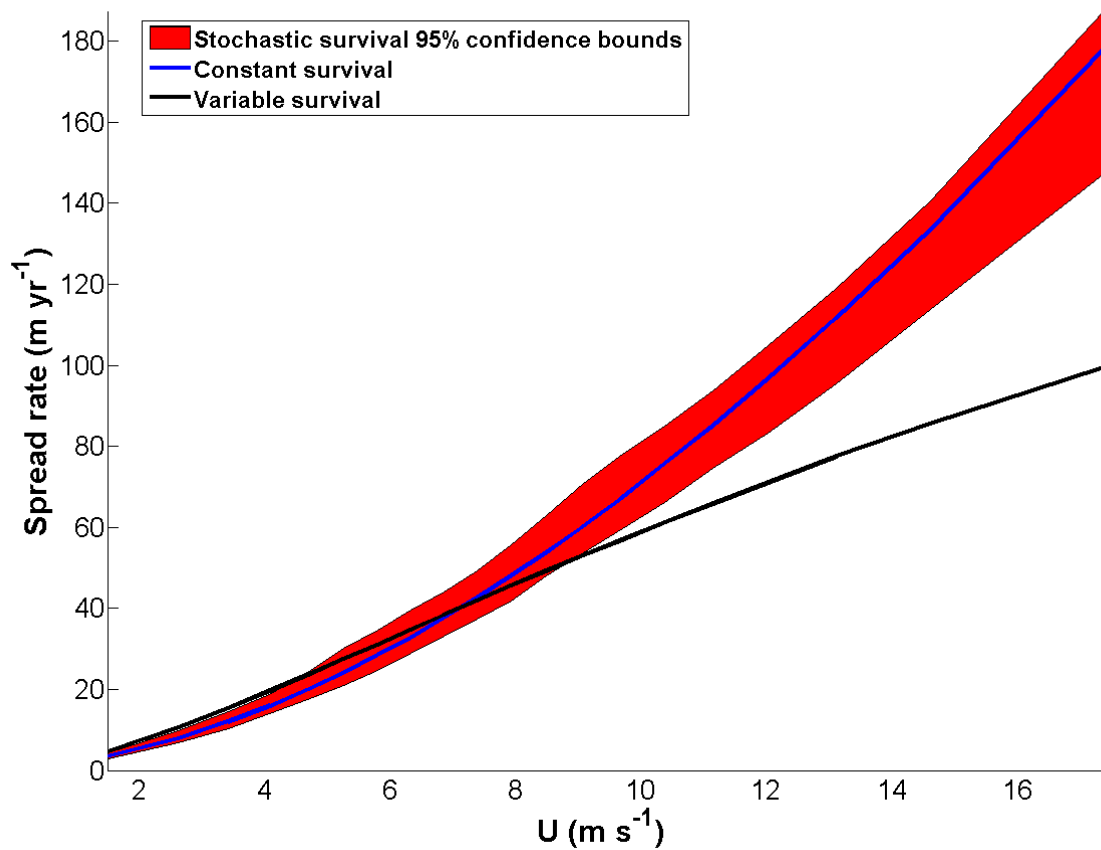


Figure S5. Stochastic bounds for spread rate of a hypothetical typical North American wind-dispersed tree species (see Figure 3 in the main text), as a function of the minimum windspeed required for seed abscission, assuming current environmental conditions scenario and relatively high mean survival. The 95% confidence intervals (red area) were calculated from 80 different realizations of a random survival function of the same overall mean ($\Phi = 0.024$) of the spatially constant one (blue line). Spread rate under the corresponding spatially variable (hump-shaped) survival is shown for comparison (black line).



References for Appendix 1

- Burton T., Sharpe D., Jenkins N. & Bossanyi E. (2001). *Wind energy handbook*. John Wiley & Sons, Chichester.
- Clark, J.S., Lewis, M. & Horvath, L. (2001) Invasion by extremes: Population spread with variation in dispersal and reproduction. *Am. Nat.*, 157, 537-554.
- De Steven D. (1991a). Experiments on mechanisms of tree establishment in old-field succession: seedling emergence. *Ecology*, 72, 1066-1075.
- De Steven D. (1991b). Experiments on mechanisms of tree establishment in old-field succession: seedling survival and growth. *Ecology*, 72, 1076-1088.
- He Y.P., Monahan A.H., Jones C.G., Dai A.G., Biner S., Caya D. *et al.* (2010). Probability distributions of land surface wind speeds over North America. *J. Geophys. Res.-Atmos.*, 115.
- Janzen D.H. (1970). Herbivores and the number of tree species in tropical forests. *Am. Nat.*, 104, 501-528.
- Katul, G.G., Porporato, A., Nathan, R., Siqueira, M, Soons, M.B., Poggi, D. *et al.* (2005) Mechanistic analytical models for long-distance seed dispersal by wind. *Am. Nat.*, 166, 368-381.
- Massman, W.J. & Weil, J.C. (1999) An analytical one-dimensional second-order closure model of turbulence statistics and the Lagrangian time scale within and above plant canopies of arbitrary structure. *Boundary Layer Meteorol.*, 91, 81-107.
- Nakišenoviš N., Alcamo J., Davis G., de Vries B., Fenham J., Gaffin S. *et al.* (2000). *Special report on emissions scenarios. A special report of Working Group III of the Intergovernmental Panel on Climate Change*. Cambridge University Press, Cambridge, UK.
- Nathan R. (2006). Long-distance dispersal of plants. *Science*, 313, 786-788.

- Nathan R. & Katul G.G. (2005). Foliage shedding in deciduous forests lifts up long-distance seed dispersal by wind. *Proc. Natl. Acad. Sci. U.S.A.*, 102, 8251-8256.
- Nathan R., Safriel U.N., Noy-Meir I. & Schiller G. (2000). Spatiotemporal variation in seed dispersal and recruitment near and far from *Pinus halepensis* trees. *Ecology*, 81, 2156-2169.
- Pryor S.C., Barthelmie R.J., Young D.T., Takle E.S., Arritt R.W., Flory D. *et al.* (2009). Wind speed trends over the contiguous United States. *J. Geophys. Res.-Atmos.*, 114.
- Stoy, P. C., Katul, G.G., Siqueria, M. B. S., Juang, J-Y, Novick, K. A. *et al.* (2006) An evaluation of models for partitioning eddy covariance-measured net ecosystem exchange into photosynthesis and respiration. *Agric. For. Meteorol.* 141, 2-18.
- Terborgh J., Pitman N., Silman M., Schichter H. & Nunez V.P. (2002). Maintenance of tree diversity in tropical forests. In: *Seed dispersal and frugivory: ecology, evolution and conservation* (eds. Levey DJ, Silva WR & Galetti M). CAB International Wallingford, UK, pp. 1-18.
- Thompson S. & Katul G. (2008). Plant propagation fronts and wind dispersal: an analytical model to upscale from seconds to decades using superstatistics. *Am. Nat.*, 171, 468-479.
- Wan H., Wang X.L. & Swail V.R. (2010). Homogenization and trend analysis of Canadian near-surface wind speeds. *J. Clim.*, 23, 1209-1225.

Appendix 2. Determinants of spread rate in North American wind-dispersed tree species

I. Global sensitivity analysis of spread determinants

To assess the relative importance of five demographic parameters (β , t_M , t_L , t_{IC} and Φ) and five dispersal parameters (\bar{U} , σ_w , v_t , h_t and p_r) in determining spread, we performed sensitivity analysis on spread rate predicted by the modified-IBE spread model (Appendix 1).

The ten parameters were varied across their observed natural range estimated from a comprehensive literature survey (Table S2). For six biological parameters (β , t_M , t_L , t_{IC} , v_t and h_t) with sufficiently large sample sizes, we fitted several probability density functions (uniform, Gaussian, negative exponential, lognormal) directly to the data (Figure S6). Distribution parameters were estimated using both the standard maximum likelihood technique and the method of moments; both approaches gave the same results. We used the Akaike's Information Criterion with a second-order correction for small sample sizes (AICc) to select the best model (Burnham & Anderson 2002). We emphasize that the histograms shown in Figure S6 serve to visualize the observed distribution and were not used to fit models to the data; the models were fitted directly to the n data points for each parameter. For the seventh biological parameter (p_r), our sample size is too small yet previous work suggested a generalization for this parameter among North American wind-dispersed tree species (see Table S2). The distributions of the two wind parameters (\bar{U} , σ_w) are explained in sections I and II of Appendix 1. The tenth and final parameter of our model (Φ) is largely unknown and is varied by 4 orders of magnitude to accommodate the range measured in very few studies (see section IV of Appendix 1).

In the first step of the global sensitivity analysis, we divided the observed range of each parameter into 20 intervals according to the assumed distribution (Table S2). In the second step, a Latin hypercube sample was generated by randomly selecting 20 hypercubes, when

each interval of each input parameter is sampled once and only once. A full factorial design would require sampling of all 20^{10} hypercubes, a logistically impossible sample size. Since the number of samples required for a Latin hypercube sample is proportional to the number of intervals and is not a function of the number of parameters, this method enables an examination of broad ranges of many parameters with high resolution. The Latin hypercube sampling (McKay et al. 1979) was preferred to other random sampling techniques as it has been shown to be very effective in sensitivity analyses (McKay et al. 1979, Helton 1993).

In the third step, the specific value of each parameter within each interval was randomly selected according to the shape of the particular distribution at this range. When the values of all parameters are specified, the response variable is calculated. Stages two and three were repeated 250 times to allow each interval of a parameter to be matched with more intervals of every other parameter. In the fourth step, the resulting 5000 samples were subjected to stepwise multiple regression. Since the relationships between the response and the input parameters are clearly nonlinear (Appendix 1), their values were rank-transformed and then tested by ordinary regression (Iman and Conover 1979). This technique is useful when the relationships between the response and input variables are nonlinear but monotonic (Iman and Conover 1979).

Results of the stepwise multiple rank regression show that within their natural range of variation, maturation age, mean survival, terminal velocity and fecundity have a large impact on spread rate distances, accounting for 67% of the variation in spread rate (Table S3). Two other factors, horizontal windspeed and tree height, added 17% to the explained variance. The contribution of inter-crop interval, standard deviation vertical windspeed, longevity and proportional height of seed release was significant but marginal, jointly adding about 6% to the explained variance. The stronger impact of variation in horizontal windspeed compared to standard deviation vertical windspeed is expected from WALD's formulation because

WALD's scale parameter includes only the former, whereas WALD's shape parameter includes a combination of the two (see Appendix 1). Altogether the ten input parameters in the model accounted for approximately 90% of the variation in spread rate.

II. Determinants of the relative response of species to future environmental changes

We tested how seven basic life history traits (β , t_M , t_L , t_{IC} , v_t , h_t and p_r), as well as two composite traits summarizing demographic (lifetime reproduction = $\beta (t_L - t_M) t_{IC}^{-1}$) or dispersal (seed flight duration = $h_t p_r v_t^{-1}$) traits, separately and jointly explain inter-specific variation in predicted future-to-present spread ratio. We found significant linear relationship with one variable (t_{IC}) and significant power-law relationship with three variables (t_{IC} , β and lifetime reproduction, Figure S7). The proportion of the explained variance (R^2) was significantly higher for the power fits for all explanatory variables, hence power-law relationship was assumed. This analysis elucidates that species with low lifetime reproduction are expected to exhibit the strongest response (i.e., spread much faster than nowadays) to the projected environmental changes (Figure S7). A model selection procedure of all possible (1-9) multivariable models based on AICc criterion showed that the combination of lifetime reproduction and three other variables (β , t_L and p_r) provides the best model (AIC = -106.9) with considerably higher proportion of explained variance (adjusted $R^2 = 0.91$) compared to the single-variable model (AICc = -93.1) including only lifetime reproduction (adjusted $R^2 = 0.58$).

References for Appendix 2

Burnham K.P. & Anderson D.R. (2002) *Model selection and multimodel inference: a practical information-theoretic approach*. 2nd edn. Springer-Verlag, New York.

Helton J.C. (1993). Uncertainty and sensitivity analysis techniques for use in performance assessment for radioactive waste disposal. *Reliability Engineering and System Safety*, 42, 327-367.

Iman R.L. & Conover W.J. (1979). The use of the rank transformation in regression. *Technometrics*, 21, 499-509.

McKay M.D., Beckman R.J. & Conover W.J. (1979). A comparison of three methods for selecting values of input variables in the analysis of output from a computer code. *Technometrics*, 21, 239-245.

Table S2. Summary of model input parameters used to for ‘the typical’ North American wind-dispersed tree species, and in the sensitivity analysis aiming to represent variation across all North American wind-dispersed tree species. All parameters expect σ_w are mean values.

Name	Parameter		Value for ‘the typical’ species	Values in sensitivity analysis		References		
	Units	Symbol		Distribution	Range	# species		
<i>Demographic parameters</i>								
Annual fecundity (in good crop years)	#seeds	β	25,000	Lognormal(9.09,1.75) [*]	300 - 450,000	22	S3, S4+S18, S7, S13	
Maturation age	yrs	t_M	25	Lognormal(2.75,0.63) [*]	3 – 60	89	S1	
Longevity	yrs	t_L	200	Uniform	70 – 450	33	S2, S4, S5, S14, S16	
Inter-crop interval (between good crops)	yrs	t_C	3	Uniform	1 – 8	89	S1	
Post-dispersal survival	%	Φ	N/A	Logarithmic	0.00001 - 0.02	N/A	See Appendix 1	
<i>Dispersal parameters</i>								
Horizontal windspeed	$m\ s^{-1}$	\bar{U}	N/A	Weibull(4.69, 2.04) [†]	0.25 – 26.47	N/A		
Standard deviation vertical windspeed	$m\ s^{-1}$	σ_w	N/A	Uniform	0.25 - 3.14	N/A		
Seed terminal falling velocity	$m\ s^{-1}$	v_t	1.0	Lognormal(0.10,0.46) [*]	0.4 - 3.4	54	S6, S8, S10- S13, S15	
Tree height	m	h_t	25	Lognormal(2.92,0.60) [*]	5 – 72	154	S1, S17	
Proportional height of seed release	%	p_r	0.70	Normal(0.70,0.15) [‡]	0.4 - 1.0	6	S9, S12, S13	

^{*}Arguments are mean and standard deviation of the variable’s natural logarithm.

[†]Arguments are scale and shape parameters

[‡]Arguments are mean and standard deviation; normal distribution assumption follows Ref. S9.

Table S3. Parameter estimates (mean values) for twelve wind-dispersed tree species selected to assess inter-specific variation in spread rate (Table 1, main text), with references.

Tree species	Species abbreviation	Fecundity (seeds tree ⁻¹ yr ⁻¹)	Maturation age (yrs)	Longevity (yrs)	Interval between good seed crops (yrs) ^{S1}	Seed terminal velocity (m s ⁻¹)	Tree height (m)	Proportional height of seed release
<i>Acer rubrum</i>	AR	21440 ^{S13}	8 ^{S4}	80 ^{S4}	1.0	0.67 ^{S13}	17.2 ^{S13}	0.66 ^{S13}
<i>Acer saccharum</i>	AS	1750 ^{S7}	40 ^{S14}	300 ^{S14}	5.0	0.82 ^{S13}	31.0 ^{S1}	0.75 ^{S9}
<i>Betula lenta</i>	BL	449940 ^{S4+S18}	40 ^{S4}	150 ^{S4}	1.5	1.60 ^{S11}	24.0 ^{S1}	0.75 ^{S9}
<i>Betula papyrifera</i>	BP	27240 ^{S7}	30 ^{S14}	120 ^{S14}	2.0	0.55 ^{S8}	21.0 ^{S1}	0.75 ^{S9}
<i>Carpinus caroliniana</i>	CC	3520 ^{S13}	15 ^{S1}	75 ^{S5}	4.0	0.98 ^{S12}	11.2 ^{S12}	0.74 ^{S12}
<i>Fraxinus americana</i>	FA	15090 ^{S13}	37 ^{S4}	260 ^{S4}	4.0	1.41 ^{S12}	18.7 ^{S12}	0.70 ^{S12}
<i>Liquidambar styraciflua</i>	LS	87330 ^{S13}	25 ^{S2}	150 ^{S2}	1.0	1.05 ^{S12}	25.6 ^{S12}	0.63 ^{S12}
<i>Liriodendron tulipifera</i>	LT	96850 ^{S13}	20 ^{S4}	200 ^{S4}	1.0	1.48 ^{S12}	26.1 ^{S12}	0.66 ^{S12}
<i>Picea glauca</i>	PG	7200 ^{S7}	25 ^{S14}	200 ^{S14}	7.5	0.62 ^{S8}	23.0 ^{S1}	0.75 ^{S9}
<i>Pinus strobus</i>	PS	65000 ^{S3}	15 ^{S14}	400 ^{S14}	6.5	0.93 ^{S8}	46.0 ^{S1}	0.75 ^{S9}
<i>Pinus taeda</i>	PT	1550 ^{S13}	7 ^{S16}	190 ^{S16}	8.0	0.70 ^{S12}	31.5 ^{S12}	0.72 ^{S12}
<i>Tilia americana</i>	TA	2330 ^{S4+S18}	30 ^{S4}	140 ^{S4}	1.0	2.92 ^{S10}	16.0 ^{S2}	0.75 ^{S9}

References for Tables S2 and S3

- S1. Bonner F.T. & Karrfalt R.P. (eds.) (2008). *The woody plant seed manual*. United States Department of Agriculture, Forest Service, Agriculture Handbook 727, April 2008, http://www.nsl.fs.fed.us/nsl_wpsm.html.
- S2. Burns R.M. & Honkala B.H. (eds.) (1990). *Silvics of North America*. USDA Forest Service, Washington, DC.
- S3. Buse L.J. (1992). *Critical silvics of white pine as related to vegetation management*. Tech. Note TN-14. Ministry of Natural Resources, Northwestern Ontario Forest Technology Development Unit, Thunder Bay, Ontario.
- S4. Clark J.S. (1998). Why trees migrate so fast: confronting theory with dispersal biology and the paleorecord. *Am. Nat.*, 152, 204-224.
- S5. Gill J.D. & Healy W.M. (1974). *Shrubs and vines for northeastern wildlife*. Gen. Tech. Rep. NE-9. US Department of Agriculture, Forest Service, Northeastern Forest Experiment Station, Upper Darby, PA.
- S6. Greene D.F. & Johnson E.A. (1993). Seed mass and dispersal capacity in wind-dispersed diaspores. *Oikos*, 67, 69-74.
- S7. Greene D.F. & Johnson E.A. (1994). Estimating the mean annual seed production of trees. *Ecology*, 75, 642-647.
- S8. Greene D.F. & Johnson E.A. (1995). Long-distance wind dispersal of tree seeds. *Can. J. Bot.*, 73, 1036-1045.
- S9. Greene D.F. & Johnson E.A. (1996). Wind dispersal of seeds from a forest into a clearing. *Ecology*, 77, 595-609.
- S10. Matlack G.R. (1987). Diaspore size, shape, and fall behavior in wind-dispersed plant species. *Am. J. Bot.*, 74, 1150-1160.
- S11. Matlack G.R. (1992). Influence of fruit size and weight on wind dispersal in *Betula lenta*, a gap-colonizing tree species. *Am. Midl. Nat.*, 128, 30-39.
- S12. Nathan R., Katul G.G., Horn H.S., Thomas S.M., Oren R., Avissar R. *et al.* (2002). Mechanisms of long-distance dispersal of seeds by wind. *Nature*, 418, 409-413.
- S13. Nathan R., Unpublished data collected at Duke Forest, NC, USA during 2000-2003.
- S14. Scheller R.M. & Mladenoff D.J. (2005). A spatially interactive simulation of climate change, harvesting, wind, and tree species migration and projected changes to forest composition and biomass in northern Wisconsin, USA. *Glob. Change Biol.*, 11, 307-321.
- S15. Siggins H.W. (1933). Distribution and rate of fall of conifer seeds. *J. Agri. Res.*, 47, 119-128.
- S16. Strauss S.H. & Ledig F.T. (1985). Seedling architecture and life history evolution in pines. *Am. Nat.*, 125, 702-715.
- S17. USDA, NRCS. 2010. The PLANTS Database (<http://plants.usda.gov>, 9 November 2010). National Plant Data Center, Baton Rouge, LA 70874-4490 USA.
- S18. Wyckoff P.H. & Clark J.S. (2005). Tree growth prediction using size and exposed crown area. *Can. J. For. Res.*, 35, 13-20.

Table S4. Stepwise multiple regression for the predicted spread rate against ten input parameters of the model (see Tables S1 and S2 for symbols).

Step	Variable entered	Adjusted R^2	Standardized regression coefficient	P
1	t_M	0.299	-0.539	< 0.0001
2	Φ	0.486	0.435	< 0.0001
3	v_t	0.582	-0.305	< 0.0001
4	β	0.671	0.305	< 0.0001
5	\bar{U}	0.762	0.304	< 0.0001
6	h_t	0.841	0.279	< 0.0001
7	t_{IC}	0.864	-0.154	< 0.0001
8	σ_w	0.882	0.133	< 0.0001
9	t_L	0.893	0.107	< 0.0001
10	p_r	0.897	0.064	< 0.0001

Figure S6. Probability density distribution of six key biological parameters affecting spread rate among North American wind-dispersed tree species. The black lines represent the best probability density function model, in terms of the AICc criterion (see text), fitted directly to the data. The histograms (columns) are given to visualize the observed density distribution, and were not used to fit the models to the data.

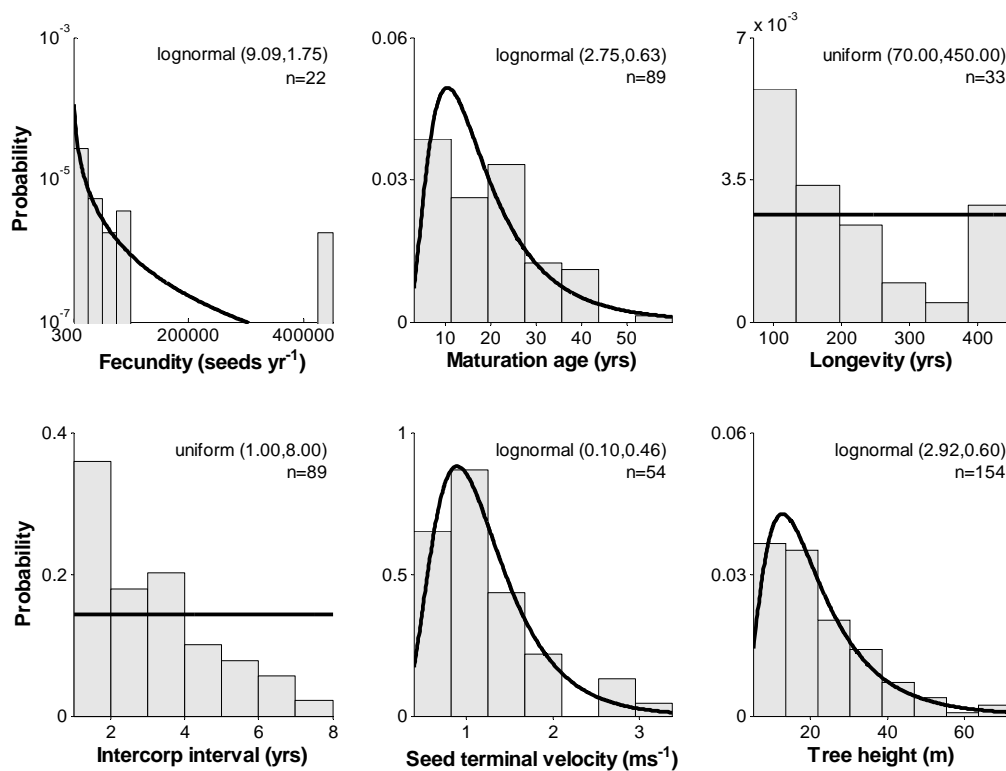
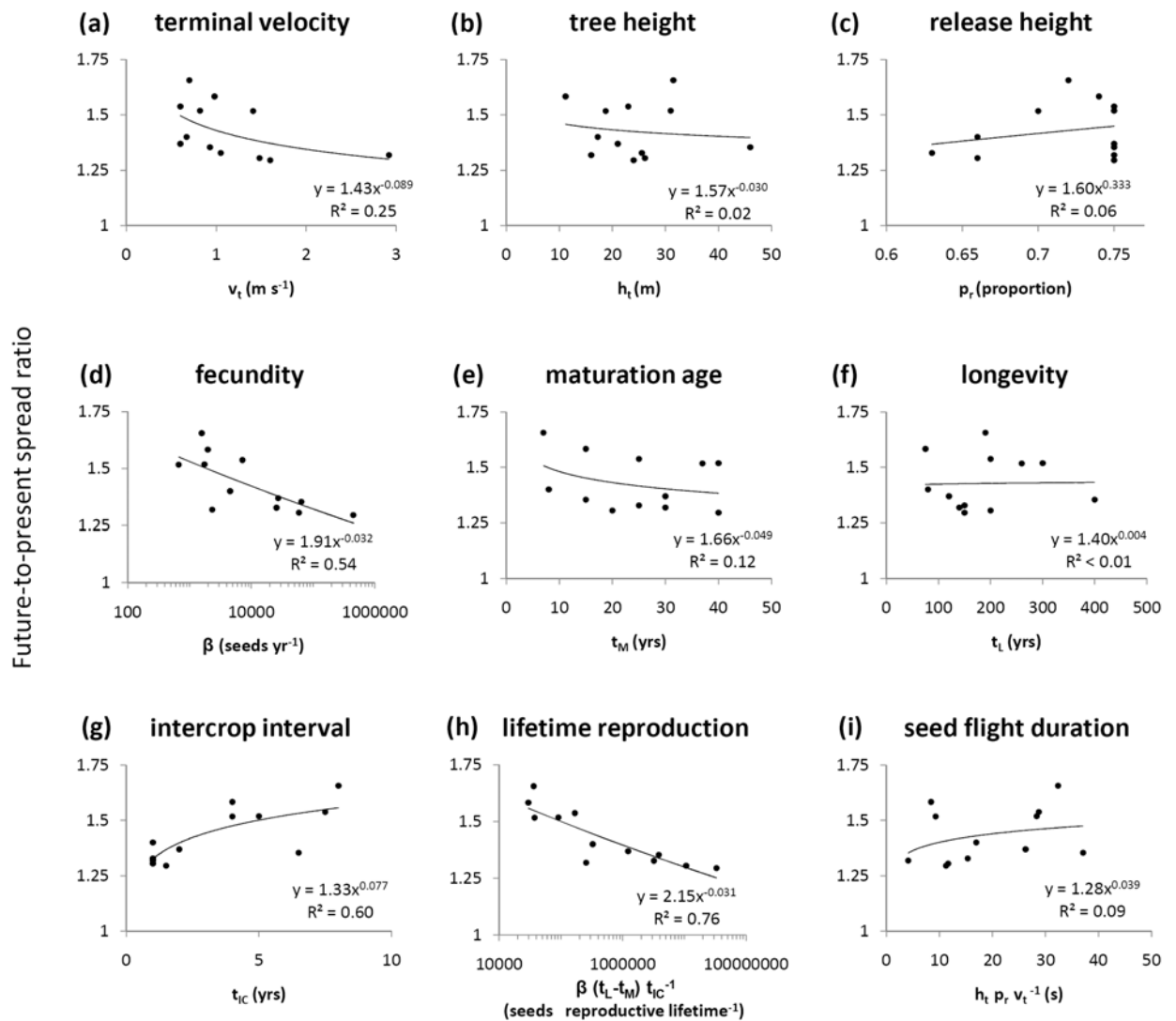


Figure S7. Predicted future-to-present spread ratio explained by inter-specific variation in current internal dispersal and demographic traits of twelve North American wind-dispersed tree species (Table 1). Explanatory variables include three dispersal parameters (a-c) and four demographic parameters (d-g), as well as two composite variables representing all demographic (h), or all dispersal (i) parameters. For each species, future-to-present spread ratios are calculated by dividing spread rate predicted for the future+ scenario (higher fecundity, earlier maturation and stronger winds) by the one predicted for the present scenario, assuming windspeed-independent seed abscission and relatively high (0.0024) and uniformly distributed mean seed-to-adult survival.



Appendix 3. Complementary analyses of current vs. future spread of North American wind-dispersed tree species.

Table S5. Full factorial analysis of spread rate in 27 scenarios representing different combinations of changes in fecundity, maturation time and surface windspeed. Negative and positive trends are, respectively, 50% and 200% of the current fecundity, 93% and 107% of the current maturation age, and 94% and 107% of the current surface windspeed. Spread rates are calculated for a typical wind-dispersed tree species (Figure 3; see Table S2 for parameter values) for three levels of survival (mean survival = 0.024, 0.00024 and 0.0000024), assuming spatially variable (hump-shaped) survival (see Appendix 1) and an intermediate minimum windspeed threshold of 3.88 m s⁻¹ for seed abscission.

Serial	Scenario name in main text	Trend			High survival		Intermediate survival		Low survival	
		Fecundity	Maturation time	Wind speed	Spread rate (m yr ⁻¹)	Rank	Spread rate (m yr ⁻¹)	Rank	Spread rate (m yr ⁻¹)	Rank
1		negative	negative	negative	54.67	20	22.68	20	1.15	20
2		negative	negative	no change	54.24	21	22.54	21	1.15	21
3		negative	negative	positive	55.10	19	22.79	19	1.15	19
4		negative	no change	negative	50.57	23	20.96	23	1.04	23
5		negative	no change	no change	50.17	24	20.83	24	1.03	24
6		negative	no change	positive	50.96	22	21.06	22	1.04	22
7		negative	positive	negative	47.03	26	19.47	26	0.93	26
8		negative	positive	no change	46.66	27	19.35	27	0.93	27
9		negative	positive	positive	47.40	25	19.57	25	0.93	25
10		no change	negative	negative	67.23	7	30.78	7	3.25	10
11		no change	negative	no change	66.68	9	30.56	10	3.24	12
12		no change	negative	positive	67.81	6	30.96	6	3.26	9
13		no change	no change	negative	62.20	14	28.46	14	2.99	14
14	Current	no change	no change	no change	61.69	15	28.25	15	2.98	15
15		no change	no change	positive	62.73	13	28.62	13	3.00	13
16		no change	positive	negative	57.86	17	26.45	17	2.77	17
17		no change	positive	no change	57.38	18	26.26	18	2.76	18
18		no change	positive	positive	58.35	16	26.61	16	2.77	16
19	Future -7	positive	negative	negative	67.23	8	30.78	8	3.25	11
20		positive	negative	no change	73.38	2	35.13	2	4.65	2
21	Future +6	positive	negative	positive	74.65	1	35.62	1	4.68	1
22		positive	no change	negative	68.46	4	32.73	4	4.30	4
23		positive	no change	no change	67.90	5	32.48	5	4.29	5
24		positive	no change	positive	69.07	3	32.94	3	4.32	3
25		positive	positive	negative	63.69	11	30.43	11	3.99	7
26		positive	positive	no change	63.16	12	30.19	12	3.97	8
27		positive	positive	positive	64.26	10	30.62	9	4.00	6

Table S6. Same as Table S5 but for three levels of minimum windspeed threshold for seed abscission: weak (0.88 m s^{-1}), intermediate (3.82 m s^{-1}), strong (8.04 m s^{-1}), assuming intermediate survival (mean survival = 0.00024).

Serial	Scenario name in main text	Trend			Weak winds		Intermediate winds		Strong winds	
		Fecundity	Maturation time	Wind speed	Spread rate (m yr^{-1})	Rank	Spread rate (m yr^{-1})	Rank	Spread rate (m yr^{-1})	Rank
1		negative	negative	negative	16.08	22	22.68	20	29.09	21
2		negative	negative	no change	16.74	20	22.54	21	29.16	20
3		negative	negative	positive	17.67	19	22.79	19	29.59	19
4		negative	no change	negative	14.87	25	20.96	23	26.87	24
5		negative	no change	no change	15.47	23	20.83	24	26.94	23
6		negative	no change	positive	16.34	21	21.06	22	27.33	22
7		negative	positive	negative	13.82	27	19.47	26	24.96	27
8		negative	positive	no change	14.38	26	19.35	27	25.02	26
9		negative	positive	positive	15.19	24	19.57	25	25.39	25
10		no change	negative	negative	21.42	11	30.78	7	40.79	11
11		no change	negative	no change	22.33	8	30.56	10	40.89	10
12		no change	negative	positive	23.66	4	30.96	6	41.61	7
13		no change	no change	negative	19.81	16	28.46	14	37.70	15
14	Current	no change	no change	no change	20.65	14	28.25	15	37.78	14
15		no change	no change	positive	21.88	10	28.62	13	38.45	13
16		no change	positive	negative	18.42	18	26.45	17	35.03	18
17		no change	positive	no change	19.20	17	26.26	18	35.11	17
18		no change	positive	positive	20.34	15	26.61	16	35.73	16
19	Future -7	positive	negative	negative	21.42	12	30.78	8	40.79	12
20		positive	negative	no change	25.46	2	35.13	2	47.74	2
21	Future +6	positive	negative	positive	27.04	1	35.62	1	48.66	1
22		positive	no change	negative	22.58	7	32.73	4	44.03	5
23		positive	no change	no change	23.55	5	32.48	5	44.12	4
24		positive	no change	positive	25.00	3	32.94	3	44.97	3
25		positive	positive	negative	20.99	13	30.43	11	40.92	9
26		positive	positive	no change	21.89	9	30.19	12	41.00	8
27		positive	positive	positive	23.25	6	30.62	9	41.79	6

Figure S8. Model results for the spread rate of twelve wind-dispersed tree species (see Table 1 for species abbreviation and parameter values). Results are presented for two extreme levels of seed abscission threshold windspeed (columns), and three levels of mean post-dispersal seed-to-adult survival (rows), across the three environmental scenarios of Figure 3 (legend in top right). Seed abscission threshold windspeed (\bar{U}_r) is 1.75 m s^{-1} (weak winds) and 16.00 m s^{-1} (strong winds). Mean survival over all space (Φ) is 0.024 (high), 0.00024 (intermediate) or 0.0000024 (low). This analysis is identical to the one presented in Figure 4, main text, but here survival is assumed to be spatially variable (hump-shaped) with the same overall mean as the spatially uniform survival assumed in Figure 4.

